Research Article

Kh. Lotfy*, Ibrahim S. Elshazly, Borhen Halouani, Saurav Sharma, Praveen Ailawalia, and Alaa A. El-Bary

Influence of Hall current and acoustic pressure on nanostructured DPL thermoelastic plates under ramp heating in a double-temperature model

https://doi.org/10.1515/phys-2025-0125
received October 02, 2024; accepted February 06, 2025

Abstract: This work explores the influence of Hall current on the thermoelastic behavior of nanostructured (nonlocal) plates made of an elastic material, modeled under a double-temperature (two-temperature theory) framework, and subjected to ramp-type heating. The dual-temperature model accounts for the separate thermal dynamics, while the nonlocal elasticity theory incorporates long-range interactions within the material, making it particularly suitable for nanoscale materials. The governing equations are derived by integrating the effects of Hall current, and nonlocal elasticity into the coupled electro-thermo-mechanical equations according to the dual-phase lag model. The solution is obtained through the application of the normal mode analysis technique, allowing for the decoupling of the governing equations into solvable ordinary differential equations. Numerical simulations are performed, and results are presented graphically to compare the wave propagation characteristics of the basic physical fields such as temperature, displacement, acoustic pressure, and stress under the influence of Hall current and varying nonlocal parameters. The results reveal significant changes in wave propagation under varying boundary conditions, offering valuable insights into the interaction between magneto-electric fields, mechanical stresses, and thermal gradients. The study provides a novel framework for understanding wave propagation in nanostructured materials and paves the way for further research into their application in advanced thermoelectric-mechanical devices.

Keywords: thermoacoustic, normal mode, the DPL model, double-temperature model, Hall current, nonlocal elasticity

* **Corresponding author: Kh. Lotfy**, Department of Mathematics, Faculty of Science, Zagazig University, P.O. Box 44519, Zagazig, Egypt, e-mail: khlotfy_1@yahoo.com
Ibrahim S. Elshazly: Department of Basic Sciences, Common First Year, King Saud University, Riyadh, 11451, Saudi Arabia, e-mail: iali2.c@ksu.edu.sa
Borhen Halouani: Department of Mathematics, College of Science, King Saud University, P.O. Box 2455, Riyadh, 11451, Saudi Arabia, e-mail: halouani@ksu.edu.sa
Saurav Sharma: University of Houston Cullen College of Engineering, 7900 Cambridge Street, #7-2G, Houston, Texas, 77054, United States of America, e-mail: sauravkuk@gmail.com
Praveen Ailawalia: Department of Mathematics, University Institute of Sciences, Chandigarh University, Gharuan-Mohali, Punjab, India, e-mail: praveen_2117@rediffmail.com
Alaa A. El-Bary: Arab Academy for Science, Technology and Maritime Transport, P.O. Box 1029, Alexandria, Egypt, e-mail: aaelbary@aast.edu
ORCID: Kh. Lotfy 0000-0001-9383-1361

Nomenclature

a	two-temperatures parameter
a_n	material constant
C_E	specific heat
e_0	material's characteristic length or intrinsic length scale
e	cubical dilatation
$e_{ij} = \frac{1}{2}(u_{i,j} + u_{j,i})$	components of the strain tensor
F_i	Lorentz force
K	thermal conductivity
l	reference length scale of the system
P	acoustic pressure
T_0	absolute temperature
t_o	pulse time rising
u_i	components of the displacement vector
α_t	coefficient of linear thermal expansion
σ_{ij}	components of the stress tensor
φ	conductive heat temperature
ρ	density of the medium
ε_0	electric permittivity
δ_{ij}	Kronecker delta function

$\lambda,\ \mu$	Lame's parameters
μ_0	magnetic permeability
$\varepsilon^2 = \sqrt{a_n e_0 / l}$	nonlocal parameter
ε_{ijr}	permutation tensor
τ_θ, τ_q	thermal relaxation time
$\theta = T - T_0$	thermodynamical temperature
$\gamma = (3\lambda + 2\mu)\alpha_t$	volume thermal expansion

1 Introduction

The interplay between the Hall current and acoustic pressure in nanostructured thermoelastic plates under ramp heating in a dual-temperature model is crucial for understanding the coupled electromechanical and thermal responses in advanced materials. The Hall current, induced by the interaction of electric and magnetic fields, modifies the charge carrier distribution and exerts a significant influence on the propagation of acoustic waves within the plate. This interaction becomes even more complex under ramp heating, which introduces a transient thermal gradient that drives thermal stresses and enhances the non-equilibrium effects described by the dual-temperature theory. In nanostructures, where size-dependent properties dominate, these effects are amplified due to the enhanced surface-to-volume ratio and quantum confinement. Investigating this problem is vital for applications in micro- and nanoscale devices, such as sensors and actuators, where precise control of thermal and electromechanical interactions is essential. Understanding these relations contributes to the design of materials and devices capable of withstanding high-frequency electromagnetic and thermal fields in emerging technologies.

The study of thermoelasticity, a fundamental area of continuum mechanics, is essential for understanding the complex interactions between thermal and mechanical processes in solid materials [1]. Classical thermoelasticity, which integrates heat conduction and elasticity, provides a foundational framework for examining how temperature changes influence mechanical deformations and vice versa [2]. However, traditional theories are often inadequate for capturing the nuances of heat transfer in scenarios involving rapid thermal transients, high-frequency oscillations, or nanoscale systems. Such limitations have driven the evolution of advanced thermoelastic theories that incorporate more realistic heat propagation mechanisms [3]. By introducing finite thermal wave speeds and addressing the temporal delay in thermal signal transmission, these extended models offer significant improvements in accurately describing non-equilibrium thermal processes [4]. This progression, marked by the transition from classical to hyperbolic and generalized thermoelasticity, has opened new avenues for studying phenomena like thermal shocks, second sound effects, and microstructural thermal inertia, which are critical in modern materials science and engineering applications [5]. The dual-phase-lag (DPL) heat conduction model, introduced by Tzou [6], revolutionized the understanding of transient thermal processes by incorporating two distinct delays: the phase lag of the heat flux and the phase lag of the temperature gradient. This approach addresses the limitations of classical Fourier heat conduction, which assumes infinite thermal propagation speed, making it unsuitable for applications involving rapid thermal responses or micro- and nanoscale systems [7]. By introducing these phase lags, the DPL model accounts for the finite relaxation times associated with heat flux and temperature gradient, providing a more accurate depiction of non-equilibrium thermal behavior.

The two-temperatures theory (2TT), initially introduced by Chen *et al.* [8], provides a framework for heat transfer in deformable materials by distinguishing between two distinct temperature fields: The thermodynamic temperature and the conductive temperature. This distinction arises from the non-equilibrium heat conduction processes that occur at small scales or under rapid thermal variations. Many authors demonstrated that when external heat sources are present, the difference between these two temperatures is proportional to the heat supply, while in the absence of external heating, the temperatures converge to equilibrium [9–11]. Quintanilla [12] investigated the mathematical and physical properties of the 2TT, including stability and spatial resolution, reinforcing its applicability to advanced thermal systems. Building on this framework, Youssef [13] proposed a generalized thermoelasticity model based on the two-temperature concept, where the relationship between the temperature difference and the heat supply is defined through a non-negative constant. Over the years, the 2TT has gained significant attention in the context of generalized thermoelasticity and extended thermodynamics, providing critical insights into heat transfer processes in nano-engineered materials and complex thermal environments [14–17]. The use of 2TT (conductive and thermodynamic temperatures) in thermoelastic models addresses this shortcoming, offering greater accuracy in describing heat transfer dynamics. On the other hand, Awad [18] introduced a novel idea about the spatial decay estimates in semi-cylindrical with bounded domains, according to the non-classical linear thermoelasticity. Awad *et al.* [19] studied a thermal resonance according to the temperature amplitude attained and oscillations for an external exciting frequency source in the electron–phonon interaction process.

In thermoelasticity, the interaction between magnetic fields and acoustic pressure plays a critical role in analyzing the dynamic behavior of materials under external influences. Magnetic fields influence the elastic properties of materials, altering the propagation of acoustic waves through magnetoacoustic coupling, a phenomenon where the Lorentz force on charged particles induces or modifies acoustic wave behavior [20]. Lotfy *et al.* [21] explored the effects of magnetic fields on photothermal transport processes in semiconducting materials, incorporating Thomson effects and microtemperature phenomena. Their research also addressed Hall current impacts in rotating semiconducting media subjected to magnetic fields and ramp heating [22,23]. Mandelis [24] employed the photoacoustic effect to study thermal waves in elastic semiconductors, expanding the understanding of energy interactions in such systems. Additionally, Lotfy *et al.* [25] proposed a model for photoacoustic and plasmaelastic interactions in nonlocal thermoelastic media, emphasizing the role of laser-induced heating and variable thermal conductivity. These studies underscore the importance of magnetoacoustic interactions in advancing technologies like magnetoacoustic imaging and the development of magnetoelastic materials [26–29]. Some theoretical studies investigate the behavior of surface wave propagation in magneto-electro-elastic structures [30]. Tiwari *et al.* [31] studied the memory response according to the DPL thermoelasticity under the nonlocal effect. Singhal [32] examined the Love-type wave velocity during imperfect interface in the context of the piezo-structure of three distinct rheological models. Gupta *et al.* [33,34] studied the two temperature theories in the context of the photo-thermo-piezo-elastic theory with fractional order in a semiconductor material. Barak *et al.* [35] analyzed the nonlocal dual-phase-lag at distinct piezo-thermoelastic media to study the behavior of higher-order heat equations and wave propagations.

The novelty of the present study lies in its comprehensive investigation of the interplay between magnetic fields, acoustic pressure, and thermoelastic effects in nonlocal elastic media under ramp heating conditions. While previous research has explored these phenomena separately, this work introduces a coupled model that integrates the effects of Hall currents, two-temperature phenomena, and magnetic field-induced acoustic wave modulation in a nonlocal elastic medium. The methodology employs a combination of analytical and numerical techniques to solve the governing equations of magneto-acoustic coupling in the context of nonlocal thermoelasticity, with particular attention to ramp heating conditions. The motivation for this research stems from the need to improve our understanding of the behavior of advanced materials under extreme thermal and electromagnetic conditions, particularly for applications in magneto-acoustic imaging, sensor technologies, and laser-induced thermal processing. However, a limitation of this study is the complexity of the coupled system, which may restrict the applicability of the model to highly idealized scenarios, potentially overlooking real-world factors such as material heterogeneities or external noise. Despite this, the insights gained provide a significant step forward in modeling and understanding the dynamic behavior of semiconducting materials in the presence of magnetic fields and thermal gradients.

2 Formulation of the problem

Through the elastic medium, the main equations that describe the interactions between acoustic, thermal, electromagnetic field, and mechanical waves can be derived by coupling the heat conduction, thermoelasticity, and wave propagation equations. The general form of the dual-phase-lag heat conduction equation with two temperatures in the presence of thermal waves is expressed as follows [23,36]:

$$K\left(1+\tau_\theta\frac{\partial}{\partial t}\right)\varphi_{,ii}-\left(\frac{\partial}{\partial t}+\tau_q\frac{\partial^2}{\partial t^2}\right)\rho C_E T + \left(\frac{\partial}{\partial t}+\tau_q\frac{\partial^2}{\partial t^2}\right)\gamma T_0 u_{i,j}=0. \tag{1}$$

For a transversely isotropic (or transversely thermoelastic) material under the influence of the Lorentz force ($F_i=\mu_0(\vec{J}\times\vec{H})$), the equation of motion in the general form can be obtained by considering both the mechanical and thermal effects, as well as the interaction between the material's deformation and the magnetic field. In such materials, the stress–strain relationships and the thermal field are coupled with the mechanical wave propagation, and the Lorentz force modifies the equations of motion by influencing the charge carriers. For the mechanical wave interactions, the displacement field u_i in the elastic medium is governed by the following nonlocal equation of motion under the effect of the Lorentz force [32,34]:

$$\rho(1-\varepsilon^2\nabla^2)\ddot{u}_i=\sigma_{ij,j}+(1-\varepsilon^2\nabla^2)F_i \quad (i,j=1,\ 2,\ 3). \tag{2}$$

In the context of the 2TT, the interaction between φ and T is described by a set of coupled differential equations that account for the heat flow and temperature gradients in the material. These equations capture the transient heat conduction process, where the difference between φ and T arises due to the lag in thermal propagation between the two temperatures. The general form of the 2TT equations is given by [13]

$$\varphi-a\varphi_{,ii}=T. \tag{3}$$

The acoustic diffusivity in the elastic medium can be characterized by the acoustic pressure or the thermoacoustic effects resulting from the heating processes. The acoustic pressure equation, which describes the interaction between acoustic pressure and temperature in a thermoelastic medium, can be derived from the fundamental principles of thermodynamics and wave propagation in the medium. In the presence of a temperature field, acoustic waves are influenced by thermal effects, and the coupling between the acoustic pressure and temperature can be modeled as follows [24–26,37]:

$$P_{,ii}(x,y,t) - \frac{1}{c_s^2}\ddot{P}(x,y,t) = \Im\beta\ddot{T}(x,y,t). \tag{4}$$

The speed of sound in the medium is c_s = 8,430 m/s. The specific heat ratio is $\Im = 1.666$ and the coefficient $\beta = 2.56 \times 10^{-6}$°C is the volumetric thermal expansion [30].

For an elastic material, the nonlocal stress–strain relation is given by [38,39]

$$\left.\begin{aligned}&(1-\varepsilon^2\nabla^2)\sigma_{ij} = \sigma'_{ij},\\&\sigma'_{ij} = \lambda e_{kk}\delta_{ij} + 2\mu e_{ij} - \gamma\left(1+\tau_\theta\frac{\partial}{\partial t}\right)T\delta_{ij}.\end{aligned}\right\} \tag{5}$$

In generalized thermoelasticity theory, the phase-lags associated with the temperature gradient and heat flux are key concepts that describe the delay in the response of thermal variables to thermal disturbances. Specifically, τ_θ and τ_q ($0 \le \tau_\theta < \tau_q$) represent the phase-lags of the temperature gradient and heat flux. The general form of the equations incorporating these phase-lags can be derived from the extended versions of the thermoelasticity theory, such as the Lord and Shulman (LS, $\tau_\theta = 0$) theory, which introduces a relaxation time for the thermal response (no phase-lags are present). The phase-lag model reflects the fact that changes in temperature and heat flux do not propagate instantaneously but rather with a delay determined by the material's thermal properties [34].

To incorporate the Hall current impact and the finite conductivity of the material into the system of equations, we need to include the generalized form of Ohm's law and the Lorentz force. The generalized Ohm's law accounts for the current density in a conducting medium, which can be influenced by both the electric field and the magnetic field (in the presence of the Hall effect). In the presence of a magnetic field, in a more general tensor form, the components of the current density tensor J_r and Lorentz force can be reformulated as follows [21,23,30]:

$$\left.\begin{aligned}&J_r = \frac{\sigma_0}{1+m^2}\left(E_i + \mu_0\varepsilon_{ijr}\left(u_{j,t} - \frac{1}{en_e}J_j\right)H_r\right)\\&F_i = \mu_0\varepsilon_{ijr}J_jH_r,\quad (i,\ j,\ r = (1=x,\ 2=y,\ 3=z)).\end{aligned}\right\} \tag{6}$$

When an elastic medium is subjected to an initial magnetic field of strength $H_r = (H_1,\ H_2,\ H_3) = (0,\ H_0,\ 0)$ along the y-axis, the electrical conductivity coefficient is denoted by $\sigma_0 = n_e t_e e_n^2/m_e$, the electron charge by e_n, and the electron mass by m_e. The density of charge carriers is represented by n_e, and t_e signifies the time between electron collisions. In this scenario, the induced electric field can be neglected to isolate the Hall effect, which arises solely due to the magnetic force. Additionally, by considering the system in two dimensions (2D), specifically within the xz-plane of the rectangular Cartesian coordinate system, the displacement vector is expressed as $\vec{u} = u_i = (u, 0, w)$. In this setup, the current density and Lorentz force components are reformulated as follows [23]:

$$\left.\begin{aligned}&J_1 = J_x = \frac{\sigma\mu_0H_0}{1+m^2}\left(m\frac{\partial u}{\partial t} - \frac{\partial w}{\partial t}\right),\\&J_3 = J_z = \frac{\sigma\mu_0H_0}{1+m^2}\left(\frac{\partial u}{\partial t} + m\frac{\partial w}{\partial t}\right),\\&F_x = -\left(\frac{\sigma_0\mu_0^2H_0^2}{1+m^2}\right)\left(\frac{\partial u}{\partial t} + m\frac{\partial w}{\partial t}\right),\\&F_z = \left(\frac{\sigma_0\mu_0^2H_0^2}{1+m^2}\right)\left(m\frac{\partial u}{\partial t} - \frac{\partial w}{\partial t}\right).\end{aligned}\right\} \tag{7}$$

The influence of the Hall current, represented by the Hall parameter $m = t_e\omega_e$, can be determined using the electron frequency $\omega_e = e\mu_0 H_0/m_e$, which is related to the parameter m.

The 2D heat Eq. (1) is reformulated as follows:

$$\begin{aligned}&K\left(1+\tau_\theta\frac{\partial}{\partial t}\right)\left(\frac{\partial^2\varphi}{\partial x^2} + \frac{\partial^2\varphi}{\partial z^2}\right)\\&= \left(\frac{\partial}{\partial t} + \tau_\theta\frac{\partial^2}{\partial t^2}\right)\rho C_E T + \gamma T_0\left(\frac{\partial}{\partial t} + \tau_\theta\frac{\partial^2}{\partial t^2}\right)\left(\frac{\partial u}{\partial x} + \frac{\partial w}{\partial z}\right).\end{aligned} \tag{8}$$

The 2D stress–strain relations are

$$(1-\varepsilon^2\nabla^2)\sigma_{xx} = (2\mu+\lambda)\frac{\partial u}{\partial x} + \lambda\frac{\partial w}{\partial z} - \gamma\left(1+\tau_\theta\frac{\partial}{\partial t}\right)T, \tag{9}$$

$$(1-\varepsilon^2\nabla^2)\sigma_{zz} = (2\mu+\lambda)\frac{\partial w}{\partial z} + \lambda\frac{\partial u}{\partial x} - \gamma\left(1+\tau_\theta\frac{\partial}{\partial t}\right)T, \tag{10}$$

$$(1-\varepsilon^2\nabla^2)\sigma_{xz} = \mu\left(\frac{\partial u}{\partial z} + \frac{\partial w}{\partial x}\right). \tag{11}$$

The 2D motion equations are

$$\begin{aligned}\rho(1-\varepsilon^2\nabla^2)\frac{\partial^2 u}{\partial t^2} &= \mu\nabla^2 u + (\mu+\lambda)\frac{\partial e}{\partial x} - \gamma\left(1+\tau_\theta\frac{\partial}{\partial t}\right)\frac{\partial T}{\partial x}\\&\quad - (1-\varepsilon^2\nabla^2)\left(\frac{\sigma_0\mu_0^2H_0^2}{1+m^2}\right)\left(\frac{\partial u}{\partial t} + m\frac{\partial w}{\partial t}\right),\end{aligned} \tag{12}$$

$$\begin{aligned}\rho(1-\varepsilon^2\nabla^2)\frac{\partial^2 w}{\partial t^2} &= \mu\nabla^2 w + (\mu+\lambda)\frac{\partial e}{\partial z} - \gamma\left(1+\tau_\theta\frac{\partial}{\partial t}\right)\frac{\partial T}{\partial z}\\&\quad + (1-\varepsilon^2\nabla^2)\left(\frac{\sigma_0\mu_0^2H_0^2}{1+m^2}\right)\left(m\frac{\partial u}{\partial t} - \frac{\partial w}{\partial t}\right).\end{aligned} \tag{13}$$

The 2D of 2TT is

$$\varphi - a\left(\frac{\partial^2\varphi}{\partial x^2} + \frac{\partial^2\varphi}{\partial z^2}\right) = T. \quad (14)$$

The 2D acoustic pressure equation can be reformulated as follows:

$$\left(\frac{\partial^2 P}{\partial x^2} + \frac{\partial^2 P}{\partial z^2}\right) - \frac{1}{c_s^2}\frac{\partial^2 P}{\partial t^2} = \Im\beta\frac{\partial^2 T}{\partial t^2}. \quad (15)$$

By introducing dimensionless field variables, the governing equations can be expressed in their dimensionless forms. The main variables are then defined through their corresponding dimensionless quantities as follows [40,41]:

$$\begin{aligned}&(x', y', u', v', \varepsilon') = c_0\eta(x, y, u, v, \varepsilon),\\&(t', \tau_\theta', \tau_{q0}') = c_0^2\eta(t, \tau_\theta, \tau_q),\\&(\theta', \phi') = \frac{(T,\phi) - T_0}{T_0},\\&\sigma_{ij}' = \frac{\sigma_{ij}}{2\mu + \lambda}, \quad P' = \frac{P}{P_0},\\&\eta = \frac{\rho C_E}{K}, \quad C_2^2 = \frac{\mu}{\rho}, \quad C_0^2 = \frac{2\mu + \lambda}{\rho},\end{aligned} \quad (16)$$

where P_0 represents the initial acoustic pressure. For simplicity, the dashes can be omitted. The core 2D equations in this case can be expressed in their dimensionless form as follows:

$$\begin{aligned}&\left(1 + \tau_\theta\frac{\partial}{\partial t}\right)\nabla^2\varphi - \left(1 + \tau_q\frac{\partial}{\partial t}\right)\frac{\partial\theta}{\partial t}\\&- \xi\left(1 + \tau_q\frac{\partial}{\partial t}\right)\frac{\partial}{\partial t}\left(\frac{\partial u}{\partial x} + \frac{\partial w}{\partial z}\right) = 0,\end{aligned} \quad (17)$$

$$\varphi - \theta = \beta\left(\frac{\partial^2\varphi}{\partial x^2} + \frac{\partial^2\varphi}{\partial z^2}\right), \quad (18)$$

$$\begin{aligned}(1 - \varepsilon^2\nabla^2)\frac{\partial^2 u}{\partial t^2} &= a_1^*\nabla^2 u + a_2\frac{\partial e}{\partial x} - a_0\left(1 + \tau_\theta\frac{\partial}{\partial t}\right)\frac{\partial\theta}{\partial x}\\&- \frac{\Gamma(1 - \varepsilon^2\nabla^2)}{1 + m^2}\left(\frac{\partial u}{\partial t} + m\frac{\partial w}{\partial t}\right),\end{aligned} \quad (19)$$

$$\begin{aligned}(1 - \varepsilon^2\nabla^2)\frac{\partial^2 w}{\partial t^2} &= a_1^*\nabla^2 w + a_2\frac{\partial e}{\partial z} - a_0\left(1 + \tau_\theta\frac{\partial}{\partial t}\right)\frac{\partial\theta}{\partial z}\\&+ \frac{\Gamma(1 - \varepsilon^2\nabla^2)}{1 + m^2}\left(m\frac{\partial u}{\partial t} - \frac{\partial w}{\partial t}\right),\end{aligned} \quad (20)$$

$$\left(\nabla^2 - \varepsilon_p\frac{\partial^2}{\partial t^2}\right)P - \eta_p\frac{\partial^2\theta}{\partial t^2} = 0, \quad (21)$$

where $\xi = \frac{\gamma}{\rho C_E}$ and $\beta = a\eta^2 c_0^2$, $a_1^* = \frac{\mu}{\rho C_0^2}$, $a_2 = \frac{\mu + \lambda}{\rho C_0^2}$, $a_0 = \frac{\gamma T_0}{\rho C_0^2}$, $\varepsilon_p = \frac{c_0^2}{c_s^2}$, $\eta_p = \frac{\Im\beta T_0 c_0^2}{P_0}$, $\Gamma = \frac{\sigma_0 C_T \mu_0^2 H_0^2}{\rho_0}$, and $\nabla^2 = \frac{\partial^2}{\partial x^2} + \frac{\partial^2}{\partial z^2}$.

Due to the various field variables that have been analyzed, we can introduce the potential functions $\Pi(x, z, t)$ and $\psi(x, z, t)$. These functions allow us to describe the acoustic waves more effectively, and the corresponding partial differential equations can be expressed as follows [42,43]:

$$u = \frac{\partial\Pi}{\partial x} + \frac{\partial\psi}{\partial z}, \quad w = \frac{\partial\Pi}{\partial z} - \frac{\partial\psi}{\partial x}. \quad (22)$$

By transforming Eq. (22) into Eqs. (17), (19), and (20), the corresponding system of equations can be formulated as follows:

$$\begin{aligned}&\left(1 + \tau_\theta\frac{\partial}{\partial t}\right)\nabla^2\varphi - \left(1 + \tau_q\frac{\partial}{\partial t}\right)\frac{\partial\theta}{\partial t} - \xi\left(\frac{\partial}{\partial t} + \tau_q\frac{\partial^2}{\partial t^2}\right)\nabla^2\,\Pi\\&= 0,\end{aligned} \quad (23)$$

$$\begin{aligned}&\left[\nabla^2 - a_3(1 - \varepsilon^2\nabla^2)\left(\frac{\partial^2}{\partial t^2} - \frac{\Gamma}{1 + m^2}\frac{\partial}{\partial t}\right)\right]\Pi\\&- a_0 a_3\left(1 + \tau_\theta\frac{\partial}{\partial t}\right)\theta = -\frac{a_3 m\Gamma}{1 + m^2}(1 - \varepsilon^2\nabla^2)\frac{\partial\psi}{\partial t},\end{aligned} \quad (24)$$

$$\begin{aligned}&\left[\nabla^2 - (1 - \varepsilon^2\nabla^2)\left(a_4\frac{\partial^2}{\partial t^2} + \frac{\Gamma}{a_1^*(1 + m^2)}\frac{\partial}{\partial t}\right)\right]\\&\times\,\psi = \frac{m\Gamma}{a_1^*(1 + m^2)}(1 - \varepsilon^2\nabla^2)\frac{\partial\Pi}{\partial t},\end{aligned} \quad (25)$$

where $a_3 = \frac{1}{a_1^* + a_2}$ and $a_4 = \frac{1}{a_1^*}$.

Eqs. (24) and (25) describe the dynamics of transverse waves in the system. These equations specifically describe transverse waves, which are independent of the overall motion and do not rely on thermal or mechanical forces. These elastic waves propagate through space, maintaining their strength throughout their journey.

3 Solution to the problem

To solve the system of governing equations, we will assume that the domain variables are evaluated using the following forms based on normal mode analysis [44,45]:

$$\begin{aligned}&[\Pi, \psi, \varphi, \theta, P, \sigma_{ij}](x, z, t)\\&= \{\Pi^*, \psi^*, \varphi^*, \theta^*, P^*, \sigma_{ij}^*\}(x)\exp(\omega t + ibz),\end{aligned} \quad (26)$$

where ω is the angular frequency of the wave, $i = \sqrt{-1}$, the propagation constant (wave number) is b, and the spatial-dependent part of each field variable, evaluated at position x are $(\Pi^*, \psi^*, \varphi^*, P^*, \theta^*)(x)$, and $\sigma_{ij}^*(x)$. Eq. (26) can be applied for the main Eqs. (18), (21) and (23)–(25), yields:

$$(D^2 - b^2)\varphi^* - A\theta^* - B(D^2 - b^2)\Pi^* = 0, \quad (27)$$

$$(\Omega_1 D^2 - A_1)\Pi^* - A_2\theta^* + B_1(\varepsilon^2 D^2 - \Omega_2)\psi^* = 0, \quad (28)$$

$$(\Omega_4 D^2 - B_2)\psi^* - B_3(\varepsilon^2 D^2 - \Omega_2)\Pi^* = 0, \quad (29)$$

$$(D^2 - A_3)\varphi^* + \beta^*\theta^* = 0, \quad (30)$$

$$(D^2 - \alpha_1)P^* - \alpha_2\theta^* = 0, \quad (31)$$

where $A = \frac{\omega(1+\omega\tau_q)}{(1+\omega\tau_\theta)}$, $B = \frac{\xi\omega(1+\omega\tau_q)}{(1+\omega\tau_\theta)}$, $\Omega_1 = 1 + a_3\varepsilon^2\vartheta_1$, $A_1 = b^2 + a_3\Omega_2\vartheta_1$, $\Omega_2 = 1 + \varepsilon^2 b^2$, $\vartheta_1 = \omega^2 + \frac{\omega\Gamma}{1+m^2}$, $A_2 = a_0 a_3(1 + \tau_\theta\omega)$, $B_1 = \frac{\omega a_3 m\Gamma}{1+m^2}$, $B_2 = (b^2(1+\varepsilon^2) - 1)\Omega_3$, $\Omega_4 = 1 + \varepsilon^2\Omega_3$, $\Omega_3 = a_4\omega^2 + \frac{\Gamma\omega}{a_1^*(1+m^2)}$, $B_3 = \frac{\Gamma m\omega}{a_1^*(1+m^2)}$ $A_3 = (\beta b^2 + 1)/\beta$, $\alpha_1 = b^2 + \varepsilon_p\omega^2$, $\alpha_2 = \eta_p\omega^2$, $\beta^* = \frac{1}{\beta}$, and $D = \frac{d}{dx}$.

The eighth-order differential equation is obtained after the elimination method is applied for Eqs. (27)–(31), one can obtain

$$(D^8 - \Theta_1 D^6 + \Theta_2 D^4 - \Theta_3 D^2 + \Theta_4)\{\varphi^*, \theta^*, \Pi^*, \psi^*, P^*\}(x) = 0, \quad (32)$$

where

$$\Theta_1 = (\Omega_4(A_4\Omega_1 + BA_2) + A_4B_1B_3\varepsilon^4)\Theta_5^{-1}, \quad (33)$$

$$\Theta_2 = \Theta_5^{-1}\begin{bmatrix}\Omega_1(A_4B_2 + A_5\Omega_1) + \Omega_4A_4(\alpha_1\Omega_1 + A)\\ + A_2B(B_2 + \Omega_4(A_3 + (\alpha_1 + b^2)))\\ + B_1B_3\varepsilon^2(\varepsilon^2(A_5 + \alpha_1A_4) + 2\Omega_2A_4)\end{bmatrix}, \quad (34)$$

$$\Theta_3 = \Theta_5^{-1}\begin{bmatrix}(\alpha_1\Omega_1 + A)(A_4B_2 + A_5\Omega_4) + B_2(A_5\Omega_1 + A_2A_3B)\\ + \alpha_1\Omega_4(A_1A_4 + A_2Bb^2) + B_1B_3(A_5\alpha_1\varepsilon^4 + A_4\Omega_2^2)\\ + A_2B(\alpha_1 + b^2)(B_2 + A_3\Omega_4) + 2B_1B_3\varepsilon^2\Omega_2(A_5 + \alpha_1A_5)\end{bmatrix}, \quad (35)$$

$$\Theta_4 = \Theta_5^{-1}\begin{bmatrix}(\alpha_1\Omega_1 + A)A_5B_2 + A_1\alpha_1(B_2A_4 + A_5\Omega_4)\\ + (\alpha_1 + b^2)A_2A_3BB_2 + 2B_1B_2\alpha_1\varepsilon^2\Omega_2A_5\\ + A_2B\alpha_1b^2(B_2 + A_3\Omega_4) + B_1B_3\Omega_2^2(A_5 + \alpha_1A_5)\end{bmatrix}, \quad (36)$$

where $A_4 = \beta^* + A$, $A_5 = \beta^* b^2 + AA_3$, and $\Theta_5 = \Omega_4(A_4\Omega_1 + A_2B) + A_4B_1B_3\varepsilon^4$.

Here is the structured presentation of the homogeneous factorization Eq. (32).

$$(D^2 - m_1^2)(D^2 - m_2^2)(D^2 - m_3^2)(D^2 - m_4^2)\{\varphi^*, \theta^*, \Pi^*, \psi^*, P^*\}(x) = 0. \quad (37)$$

This transforms the equation into the characteristic equation with roots m_n^2 $(n = 1, 2, 3, 4)$

$$m^8 - \Theta_1 m^6 + \Theta_2 m^4 - \Theta_3 m^2 + \Theta_4 = 0. \quad (38)$$

The linear solutions are formulated from exponential solutions. The general solution is obtained when $x \to \infty$ as follows:

$$(P^*, \theta^*, \varphi^*, \Pi^*, \psi^*)(x) = \sum_{n=1}^{4}(1, \ \Gamma_{1n}, \ \Gamma_{2n}, \ \Gamma_{3n}, \ \Gamma_{4n})D_n \exp(-m_n x), \quad (39)$$

where D_n is a constant determined by boundary conditions and

$\Gamma_{1n} = \frac{(m_n^2 - \alpha_1)}{\alpha_2}$, $\Gamma_{2n} = -\frac{\Gamma_{1n}\beta^*}{m_n^2 - A_3}$, $\Gamma_{3n} = -\frac{(m_n^2 - \alpha_1)(A_4m_n^2 - A_5)}{\alpha_2B(m_n^2 - A_3)(m_n^2 - b^2)}$, $\Gamma_{4n} = -\frac{B_3(m_n{}^2 - \alpha_1)(\varepsilon^2 m_n{}^2 - \Omega_2)(A_4m_n^2 - A_5)}{\alpha_2B(m_n^2 - A_3)(\Omega_4m_n^2 - B_2)(m_n^2 - b^2)}$.

The strain–displacement components are generally derived from Eq. (22) as follows:

$$u^*(x) = D\Pi^* + ib\,\psi^* = \sum_{n=1}^{4}(-\Gamma_{3n}m_n + ib\Gamma_{4n})D_n e^{-m_n x}, \quad (40)$$

$$w^*(x) = ib\Pi^* - D\psi^* = \sum_{n=1}^{4}(\Gamma_{4n}m_n + ib\Gamma_{3n})D_n e^{-m_n x}. \quad (41)$$

Utilizing Eqs. (39), (41), and (42) to obtain the stress components from the constitutive relations

$$\sigma_{xx}^* = \sum_{n=1}^{4} h_n D_n \exp(-m_n x), \quad (42)$$

$$\sigma_{yy}^* = \sum_{n=1}^{4} h_n' D_n \exp(-m_n x), \quad (43)$$

$$\sigma_{xy}^* = \sum_{n=1}^{4} h_n'' D_n \exp(-m_n x), \quad (44)$$

where

$$h_n = \Gamma_{3n}m_n^2 - ibm_n\Gamma_{4n} + \frac{ib\lambda(\Gamma_{4n}m_n + ib\Gamma_{3n})}{2\mu + \lambda} - \frac{\gamma\Gamma_{1n}(1 + \tau_\theta\omega)T_0}{2\mu + \lambda}, \quad (45)$$

$$h_n' = (ib\Gamma_{4n}m_n + b^2\Gamma_{3n}) + \frac{\lambda(ibm_n\Gamma_{4n} - \Gamma_{4n}m_n^2)}{2\mu + \lambda} - \frac{\gamma\Gamma_{1n}(1 + \tau_\theta\omega)T_0}{2\mu + \lambda}, \quad (46)$$

$$h_n'' = \frac{-\mu}{2\mu + \lambda}(\Gamma_{4n}(m_n^2 + b^2) + 2ibm_n\Gamma_{3n}). \quad (47)$$

4 Boundary conditions

To solve the presented system of differential equations and determine the unknown parameters $M_n (n = 1, \ 2, \ 3, \ 4)$ discussed in Section 2, certain boundary conditions for the problem under investigation can be provided. In this study, we examine a thermally elastic quasi-space subjected to mechanical stress and acoustic pressure on its surface, influenced by a temperature gradient of the ramp type, all under the effects of a magnetic field and Hall current at $x = 0$ for a nonlocal elastic medium. Consequently, the following boundary conditions are considered [46–48]:

(1) Ramp-type heating (varies sinusoidally with time) is applied based on thermal conditions with an arbitrary constant temperature θ_1, determined by the heating rise time or the sinusoidal pulse width t_0, which is considered on the outer surface [46].

$$\theta(0, z, t) = \theta_1 \sin\left(\frac{\pi t}{t_0}\right)\exp(\omega t + ibz). \quad (48)$$

Sinusoidal time variations allow for studying the transient heat transfer behavior in materials or structures, where thermal effects are not constant but vary periodically. This helps to analyze the thermal responses which means how the material or structure responds to oscillating heat inputs, which can lead to phenomena like thermal resonance, cyclic expansion, and contraction.

(2) The Mechanical boundary condition which describes how the material interacts with its surroundings can be taken with constant magnitude force load Ω_1 for normal stress as [1,2]

$$\sigma_{xx}(0,\ z,\ t) = \Omega_1(z,\ \ t) = -\Omega_1^* \exp(\omega t + ibz). \quad (49)$$

(3) The tangent mechanical stress can be chosen as zero traction (free surface) as follows:

$$\sigma_{xy}(0, z, t) = 0. \quad (50)$$

(4) Acoustic pressure refers to the fluctuating pressure within a medium caused by the propagation of acoustic waves, which result from disturbances such as sound, vibrations, or thermal gradients. At the free surface of an elastic medium, the acoustic pressure is typically related to external disturbances P_0^* which can be chosen in the form of sinusoidal acoustic pressure and is commonly used in cases where the pressure is oscillatory [31].

$$P(0, y, t) = P_0^*\ \sin(\omega t)\exp(\omega t + ibz). \quad (51)$$

By applying the normal mode method to Eqs. (48)–(51), the following system of equations was obtained:

$$\sum_{n=1}^{4}\Gamma_{1n}D_n = \theta_1 \sin\left(\frac{\pi t}{t_0}\right), \quad (52)$$

$$\sum_{n=1}^{4} h_n D_n = -\Omega_1^*, \quad (53)$$

$$\sum_{n=1}^{4} h_n'' D_n = 0, \quad (54)$$

$$\sum_{n=1}^{4} D_n = P_0^* \sin(\omega t). \quad (55)$$

The parameters $D_n (n = 1,\ 2,\ 3,\ 4)$ can be determined once the equations mentioned above are solved. As a result, the various physical fields involved have been obtained, and the entire system of equations has been resolved.

5 Validation

5.1 DPL thermoelasticity theory

When the conductivity temperature φ is equivalent to the temperature T, the DPL thermoelasticity model can be obtained (*i.e.*, $\varphi = T$). In this case, the heat equation takes the following form [6,7]:

$$K\left(1 + \tau_\theta\frac{\partial}{\partial t}\right)T_{,ii} - \left(\frac{\partial}{\partial t} + \tau_q\frac{\partial^2}{\partial t^2}\right)\rho C_E T + \left(\frac{\partial}{\partial t} + \tau_q\frac{\partial^2}{\partial t^2}\right)\gamma T_0 u_{i,j} = 0. \quad (56)$$

5.2 Influence of Hall current parameter

The proposed set of equations addresses the DPL thermoelasticity theory, capturing the interaction between elastic, thermal, and mechanical waves while neglecting the effects of external magnetic fields. To validate the model and its implementation, by neglecting the Lorentz force $\vec{F}$, the equations were reduced to the classical formulation of the nonlocal DPL thermoelasticity. This reduction was verified numerically and analytically, yielding results consistent with established literature in conventional thermoelastic models (Figure 1). In this case, the motion equation takes the form [34]

$$\rho(1 - \varepsilon^2\nabla^2)\ddot{u}_i = \sigma_{ij,j}. \quad (57)$$

5.3 Non-local impact

The formulated fundamental equations incorporate nonlocal effects to study their impact on the main physical fields in the context of thermoelastic wave propagation. To validate the robustness of the model, the following methodologies were employed:

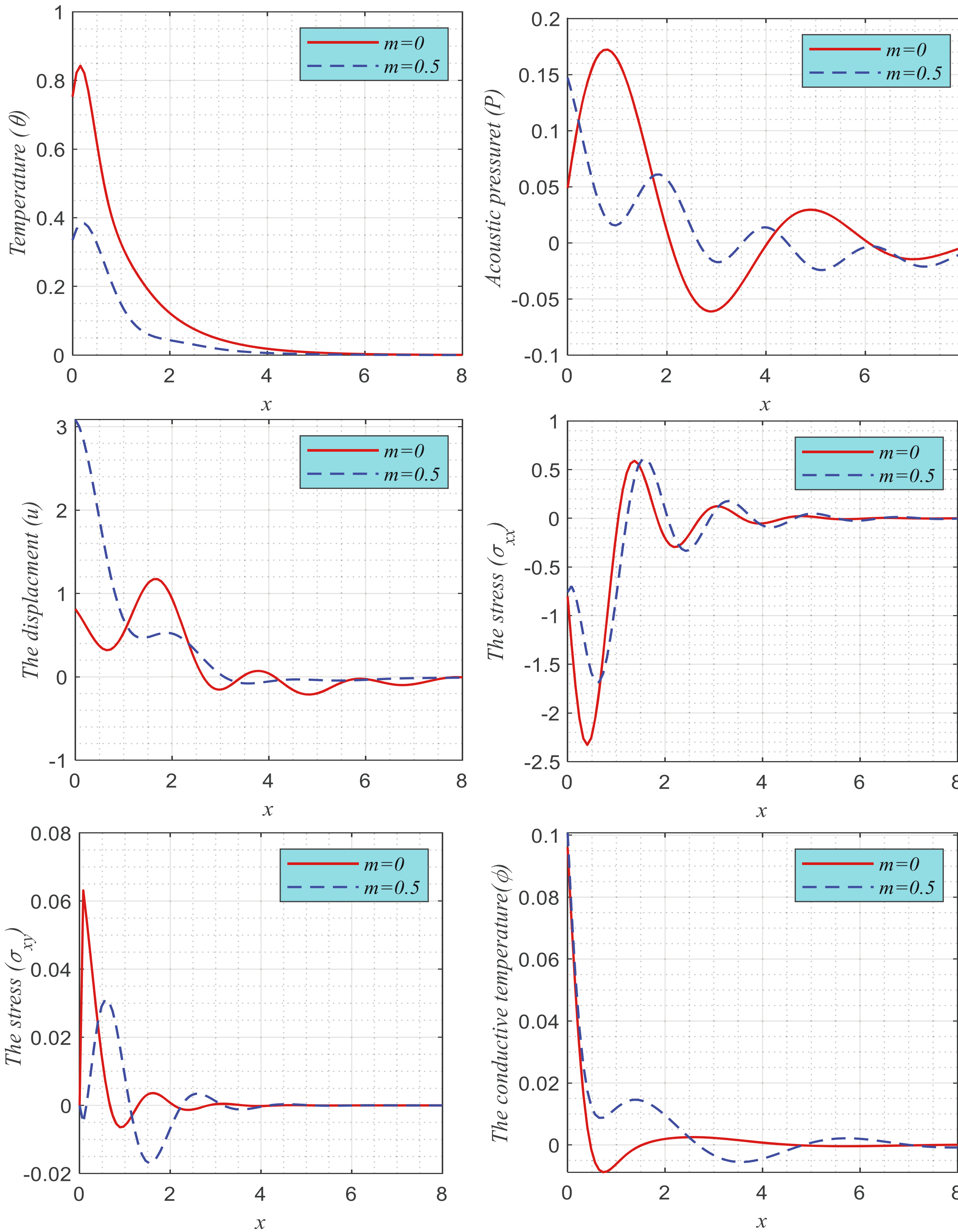

Figure 1: Variation in the primary dimensionless nonlocal physical fields for the vertical distance for two different values of the Hall current parameter, based on the DPL model, with varying sinusoidal heating parameters.

Reduction to the DPL thermoelasticity model, by setting the nonlocal parameter to zero ($\varepsilon = 0$), the equations transform into the DPL thermoelasticity model under the influence of Hall's current theory. Numerical results obtained from this limiting case were benchmarked against previously established results for the DPL framework, demonstrating a high degree of consistency and confirming the accuracy of the model reduction (Figure 2). In this case, the motion equation takes the form

$$\rho \ddot{u}_i = \sigma_{ij,j} + F_i \quad (i,\ j = 1,\ 2,\ 3). \tag{58}$$

6 Numerical results

This section provides a quantitative assessment of the analytical solutions to the various problem areas discussed earlier. This section presents numerical results for several dimensionless physical quantities associated with thermoelastic behavior, emphasizing temperature, acoustic pressure, and stress. The numerical results are presented graphically and analyzed theoretically. To highlight the influence of each factor in facilitating wave propagation within an elastic medium, a detailed discussion and analysis of its effect on the system of equations is conducted. While additional variables were chosen individually, all studies were completed within a relatively short time period ($t = 0.001$ s) when $z = -1$. To improve the comprehension of the thermoacoustic mathematical model and its theoretical outcomes, the actual values of the physical variables were considered. MATLAB (2022a) software was used to perform the numerical computations. For reference, the physical properties of copper crystals were utilized, with the material properties of copper (Cu) measured in International System (SI) units and reported as follows [31–34]:

$\lambda = 7.59 \times 10^9$ N/m^2, $\mu = 3.86 \times 10^{10}$ kg/ms^2, $\rho =$ 8,960 kg/m^3, $\tau_0 = 0.02$ s, $\alpha = -1.28 \times 10^9$ N/m^2, $\beta = 0.32 \times 10^9$ N/m^2, $\eta = 8886.73$ m/s^2, $\varepsilon = 0.0168$, $\alpha_t = 1.78 \times 10^{-5}$ K^{-1}, $k = 386$ W m^{-1} K^{-1}, $b = 1$, $C_E =$ 383.1 J/(kgk), $T_0 = 298$ K, $y = -1$, $\Omega_1^* = 0.5$, $\theta_1 = 300$ K, $P_0^* = 2$, $\omega_0 = 2$, and $\xi = 1$, where $\omega = \omega_0 + i\xi$ and $e^{\omega t} = e^{\omega_0 t}(\cos \xi t + i \sin \xi t)$. When the time is very small, the value of ω is given in real [35,36].

6.1 Hall current effect

Figure 1 illustrates the effect of the Hall current (represented by the parameter $m = 0$ for no Hall current effect and $m = 0.5$ for the Hall current effect) on the propagation of dimensionless physical fields within a nonlocal medium, based on the DPL model. It displays several key physical fields across a range of values for the vertical distance x, showing how Hall current influences the wave behavior in this nonlocal semiconductor medium. The temperature distribution appears to be highly sensitive to the presence of the Hall current. For $m = 0$, the temperature decays relatively smoothly, whereas for $m = 0.5$, the temperature exhibits more abrupt changes and a steeper decay near the origin. This could indicate that the Hall current has an intensified impact on the thermal distribution in the semiconductor, potentially linked to altered heat transport or localized heating effects due to the electronic interactions with the Hall current. The elastic (displacement) and acoustic fields variation appears to be significantly influenced by the Hall current. For $m = 0$, the acoustic field exhibits oscillations, but these oscillations are more pronounced and less symmetric for $m = 0.5$. This suggests that the Hall current introduces additional perturbations in the wave propagation, which could alter the overall dynamics of acoustic waves in the medium. The stress fields show a clear difference between the two Hall current values, with more pronounced oscillations at $m = 0.5$. The amplitude of the stress field increases when the Hall current is present, indicating that the wave propagation leads to greater internal forces in the material. This could relate to the internal material response to the coupled thermo-electro-mechanical effects, especially under external influences such as Hall currents. Thermal conductivity shows a similar pattern, where the presence of the Hall current (with $m = 0.5$) causes a sharper decline in conductivity in the initial region compared to when $m = 0$. This could suggest that Hall currents modify the way heat flows through the material, possibly due to changes in carrier mobility and heat dissipation mechanisms. The overall trend in Figure 1 highlights the significant role that Hall currents play in modifying wave propagation and thermal effects in a nonlocal medium. As m increases, the presence of Hall current introduces non-negligible changes in the acoustic, stress, temperature, and thermal conductivity fields. This suggests that Hall currents are not just a secondary effect but can substantially influence the material response to acoustic, and thermal waves in an elastic media. In the context of wave propagation, the Hall current could be interacting with the material's charge, altering their motion and consequently affecting the propagation characteristics of both acoustic and thermal waves. The nonlocal nature of the medium means that these interactions are spread over a range of distances, not localized to a point, and Hall current could introduce phase lags or shifts in the waves' behavior.

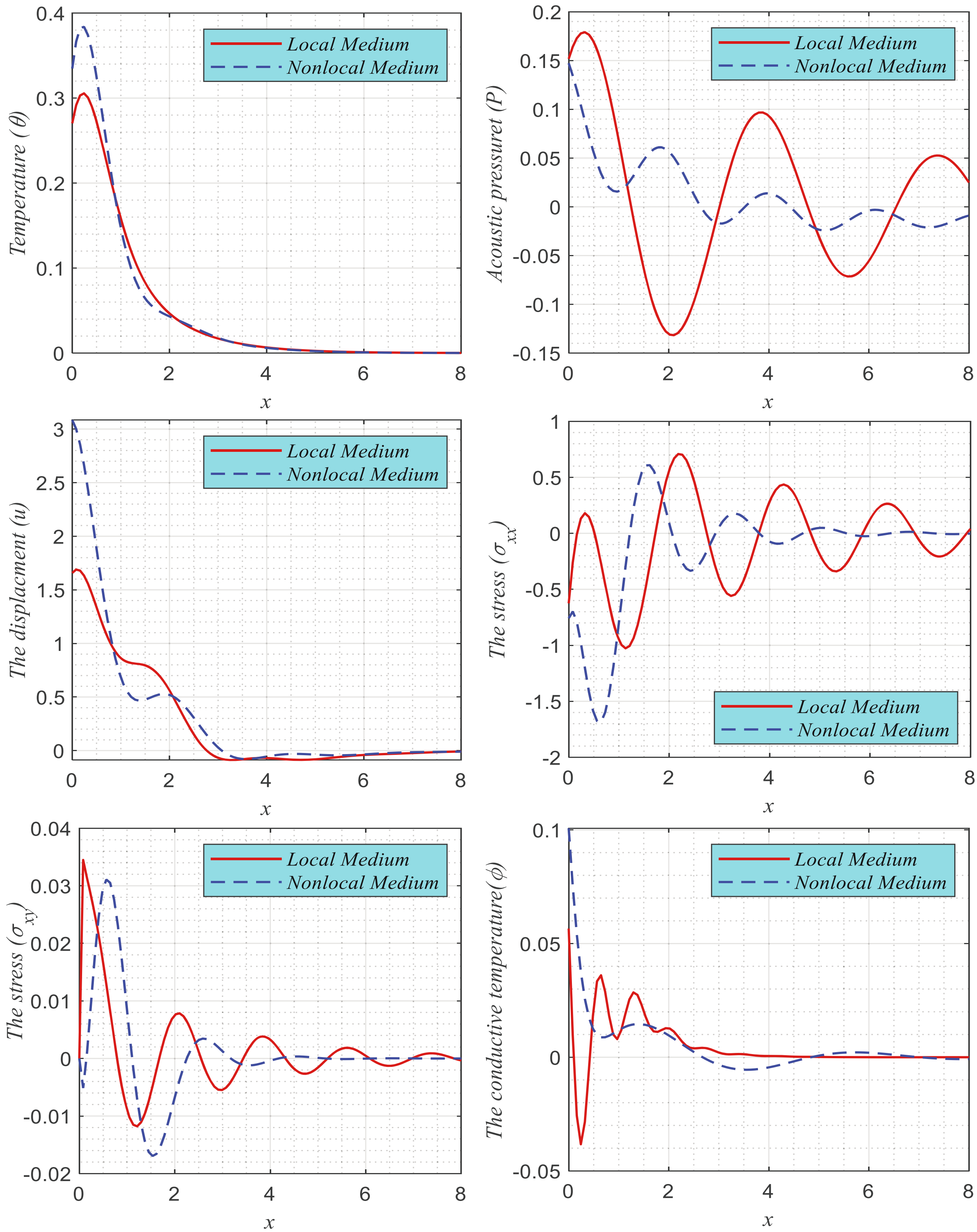

Figure 2: Variation in the primary dimensionless physical fields for the vertical distance for local and nonlocal media under the impact of Hall current, based on the DPL model, with varying sinusoidal heating parameters.

6.2 Influence of the nonlocal parameter

Figure 2 displays the influence of the nonlocal parameter on wave propagation in the context of an elastic medium under the effect of the Hall current, modeled according to the DPL approach, which leads to significant alterations in the behavior of various physical fields. This effect appears when the nonlocal parameter affects the dimensionless physical fields: Temperature, acoustic pressure, displacement, normal stress, tangent stress, and conductive temperature. When the nonlocal parameter is introduced, the temperature distribution in the medium changes due to the memory effect of the material. In the local model, the temperature evolves based on the present state of the system, while in the nonlocal case, it is affected by the past thermal history (due to phase lags). This results in more complex thermal waves, which may show delayed responses or oscillatory behavior. The nonlocal parameter models the delay in the thermal response. The inclusion of nonlocal effects tends to dampen the amplitude of acoustic pressure waves and may cause a phase shift. The nonlocal medium takes into account the history of the stress field, leading to a more gradual response rather than the sharp propagation seen in the local case. The nonlocal parameter introduces a lag in the acoustic wave's response to external excitations, modifying the pressure wave's amplitude and velocity. Displacement waves (acoustic waves) in a nonlocal medium tend to exhibit more complex patterns due to the delayed material response. These waves can show oscillations that differ from the traditional propagation in the local medium. The amplitude of displacement might also be reduced as the nonlocal effects lead to additional damping. Normal stress, which relates to the force per unit area acting perpendicular to a surface in the medium, is influenced by the nonlocal parameter by showing more complex distribution patterns. The stress response becomes less sharp and more distributed as the material "remembers" prior deformations. The inclusion of the Hall current in this context can induce additional stress components in the material, which interact with the wave propagation. Tangent stress, which is parallel to the surface of the material, behaves similar to normal stress under nonlocal effects, showing more gradual variations. Nonlocality induces additional damping or phase shifts in tangent stresses, particularly in regions where the stress concentrations would typically occur. Conductive temperature shows significant changes with nonlocal parameters because the heat conduction becomes delayed, and the temperature profile will not follow a simple gradient in time and space. This effect is more pronounced when Hall currents influence the electron transport, as they modify how energy is transferred in the medium. Finally, nonlocal parameters introduce delays or phase lags in the response of all the physical fields. The material's history influences wave propagation, temperature, stress, and displacement [31].

6.3 Impact of DPL thermal times

The relaxation times in the LS model and the DPL model play a crucial role in the propagation of waves in a nonlocal medium, especially under the influence of the Hall current which is obtained in Figure 3. These models introduce memory effects or time lags into the material's response to mechanical and thermal disturbances, which are essential for accurately modeling complex phenomena in materials with thermal and elastic relaxation processes. The LS model introduces thermal relaxation time ($\tau_\theta = 0$), which governs the delay in the heat conduction process. As the relaxation time increases, the material's thermal response becomes more sluggish, with delayed heat conduction and diffusion. The Hall current, which induces an additional electromagnetic force on charge carriers, will affect the efficiency of heat generation and transport in the medium. Thus, a longer relaxation time would cause the temperature wave to propagate more slowly and with greater damping, as the material lags in responding to thermal changes. In the DPL model ($0 \le \tau_\theta < \tau_q$), there are two relaxation times: one for the thermal flux (related to heat conduction) and another for the temperature gradient (related to the rate of change of temperature). Both relaxation times induce a phase lag in the thermal response, which causes the temperature wave to propagate with delayed changes in both the temperature and heat flux. Relaxation times in the thermal field represent the material's ability to respond to temperature changes. Longer relaxation times imply a slower response to thermal gradients, meaning heat propagation is delayed and dampened. When Hall current is present, charge carriers are driven by electromagnetic forces, further complicating the thermal behavior due to altered energy dissipation and conduction. Relaxation times control how quickly the material responds to thermal and mechanical disturbances, with larger times causing delayed, damped, or oscillatory wave propagation in all fields.

6.4 Surface wave propagation

The surface wave propagation of various dimensionless nonlocal physical fields (temperature, acoustic pressure,

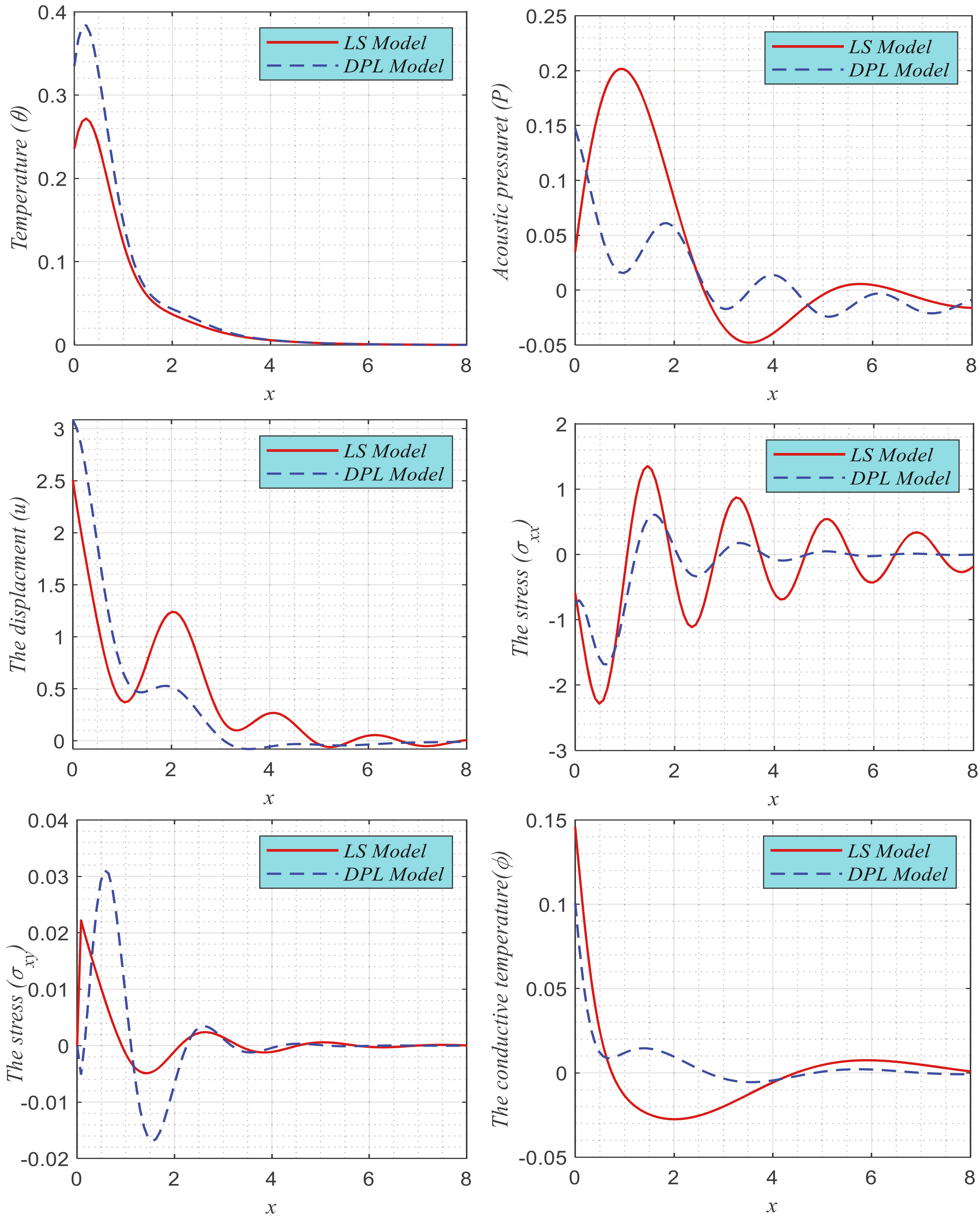

Figure 3: Variation in the primary dimensionless nonlocal physical fields for the vertical distance for different thermal memories according to the LS model and DPL model, based on the Hall current model, with varying sinusoidal heating parameters.

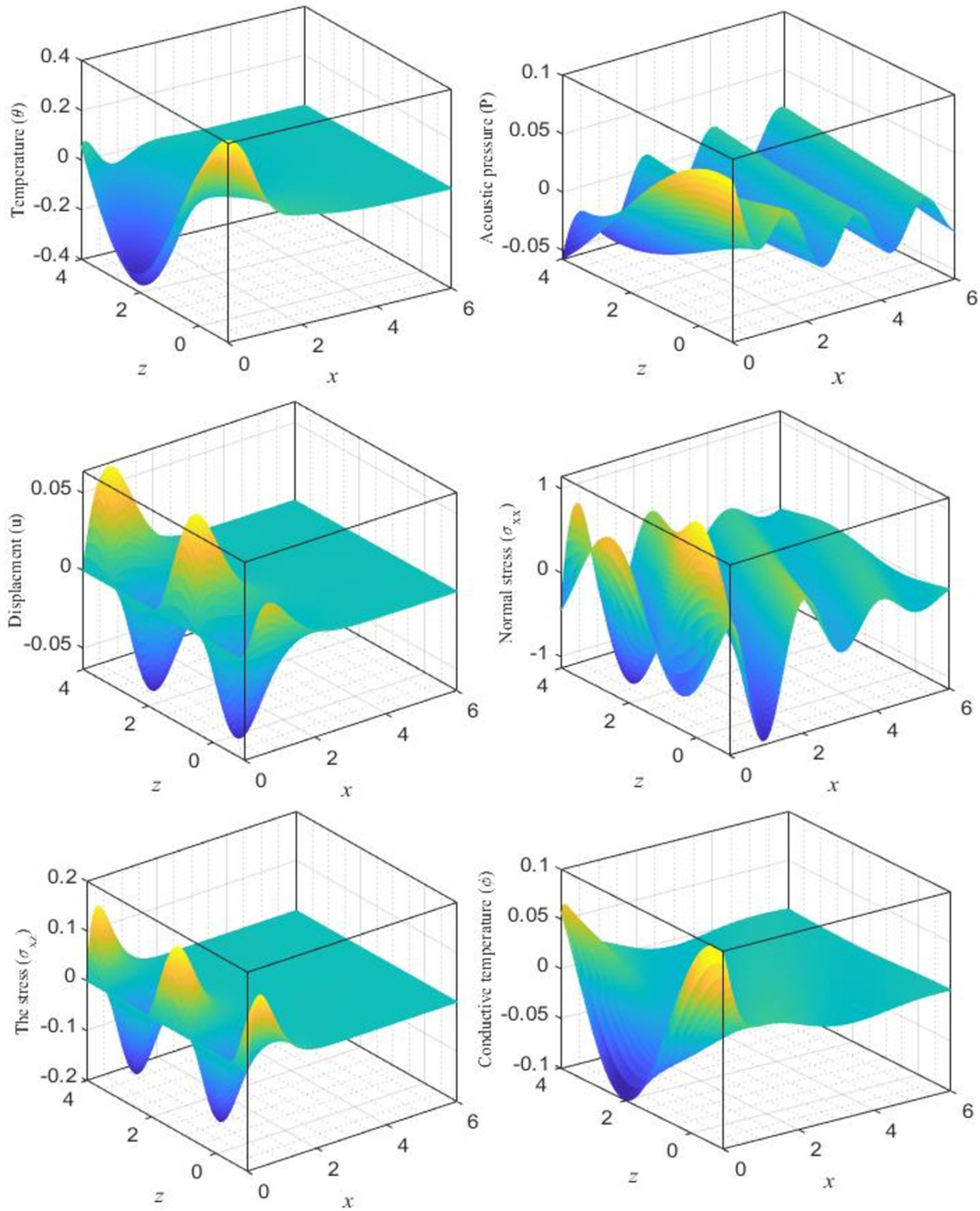

Figure 4: Variation in the primary dimensionless nonlocal physical fields for the horizontal and vertical distances according to the DPL model, based on the Hall current model, with varying sinusoidal heating parameters.

displacement, normal stress, tangent stress, and conductive temperature) is influenced by several factors. In the context of Figure 4, the DPL model and the Hall current model are used to describe the effects of sinusoidal heating on wave propagation. The figure likely shows the behavior of these fields as a function of both vertical (x) and horizontal (z) distances, while varying sinusoidal heating parameters (amplitude, frequency, or other characteristics). Let us break down the effects in detail. Sinusoidal heating typically involves a periodic temperature variation that can significantly affect the propagation of waves. In this case, the sinusoidal heating parameters influence the material's response, modifying the characteristics of wave propagation, especially in terms of amplitude, frequency, and damping. Overall, the combined effects of sinusoidal heating, Hall current, and the DPL model lead to more complex and slower wave propagation, with significant changes in the amplitude, phase, and damping of the waves.

7 Life applications

- The DPL thermoelasticity theory and its extension to nonlocal effects provide insights into heat transfer and stress distribution in nanostructures. These results are critical for developing efficient thermal management strategies in microelectronics and photonics.
- The study of elastic and thermal wave propagation with nonlocal effects can advance acoustic wave applications, such as surface acoustic wave devices, which are used in sensors, filters, and signal processing systems in communication technology.
- The framework developed in this work provides a foundation for studying mechanical and thermal behaviors in advanced materials, including nanocomposites and metamaterials. The incorporation of nonlocal effects is particularly relevant for understanding and designing materials with tailored properties at the nanoscale.
- In aerospace engineering, where materials are exposed to extreme thermal and electromagnetic environments, this study provides essential tools for predicting material behavior and ensuring reliability in advanced structural applications.
- The coupling between thermal, elastic, and electromagnetic fields can be exploited in piezoelectric and thermoelectric energy harvesting systems. Insights from this investigation could contribute to the efficiency and miniaturization of such systems.

8 Conclusion

This work presents an advanced model of magnetothermal elasticity, incorporating acoustic pressure and extending the heat transfer concept to include both dynamic and conductive temperatures, along with relaxation times. The governing equations were derived from the nonlocal thermoelastic model influenced by acoustic pressure in the presence of a strong magnetic field. The model was solved using the harmonic wave method, with specific boundary conditions applied to the free surface. The study focused on the response of nonlocal thermoelastic materials to thermal and acoustic stresses, temperature variations, and deformations, while also considering the impact of Hall effect. The role of the Hall current is emphasized, as the variations in conductivity caused by a strong magnetic field make it a significant factor. This current is generated when ions and electrons collide and move perpendicular to the electromagnetic fields along the magnetic lines of force. The current DPL model is found to offer more accurate predictions compared to the LS models, highlighting the importance of incorporating different relaxation times for a better understanding of heat and stress propagation dynamics within materials. Additionally, the varied heating sinusoidally (ramp heating) with time parameter is identified as a crucial factor in determining how heat is applied to the thermoelastic medium over time, significantly affecting the behavior of the studied thermophysical domains. Integrating the Hall current effect, varying relaxation times, and ramp-type heating parameters into thermoelastic models not only deepens our understanding of wave propagation phenomena but also facilitates the development of advanced materials and technologies. This enhanced understanding has wide-ranging implications across fields such as science, engineering, and medicine, particularly in the design of magnetostrictive materials for sensors and actuators. Furthermore, it aids in optimizing material processing techniques to improve performance and efficiency, especially in the context of tailored materials with specialized functionalities. Understanding the complex interactions between magnetic fields, thermal properties, and mechanical responses is essential for the advancement of next-generation materials.

Acknowledgments: The authors would like to extend their sincere appreciation to Researchers Supporting Project number (RSPD2025R1112), King Saud University, Riyadh, Saudi Arabia.

Funding information: Researchers Supporting Project number (RSPD2025R1112), King Saud University, Riyadh, Saudi Arabia.

Author contributions: All authors have accepted responsibility for the entire content of this manuscript and approved its submission.

Conflict of interest: The authors state no conflict of interest.

Data availability statement: The datasets generated and/or analyzed during the current study are available from the corresponding author on reasonable request.

References

[1] Biot MA. Thermoclasticity and irreversible thermodynamics. J Appl Phys. 1956;27:240–53.
[2] Hetnarski R, Ignaczak J. Generalized thermoelasticity. J Therm Stress. 1999;22:451–76.
[3] Lord HW, Shulman Y. A generalized dynamical theory of thermo-lasticity. J Mech Phys Solids. 1967;15:299–309.
[4] Green AE, Lindsay KA. Thermoelasticity. J Elast. 1972;2:1–7.
[5] Green AE, Naghdi P. Thermoelasticity without energy dissipation. J Elast. 1993;31:189–208.
[6] Tzou D. Experimental support for the lagging behavior in heat propagation. J Thermophys Heat Transf. 1995;9:686–93.
[7] Tzou D. Macro-to microscale heat transfer: the lagging behavior. Washington, DC, USA: Taylor and Francis; 1996.
[8] Chen P, Gurtin M, Williams W. On the thermodynamics of non-simple elastic materials with two temperatures. Z Angew Math Phys. 1969;20:107–12.
[9] Chen P, Williams W. A note on non-simple heat conduction. Z Angew Math Phys. 1968;19:969–70.
[10] Lotfy K. Mode-I crack in a two-dimensional fibre-reinforced generalized thermoelastic problem. Chin Phys B. 2012;21(1):014209.
[11] Othman M, Lotfy Kh. The effect of magnetic field and rotation of the 2-D problem of a fiber-reinforced thermoelastic under three theories with influence of gravity. Mech Mater. 2013;60:129–43.
[12] Quintanilla R. On existence, structural stability, convergence and spatial behavior in thermoelasticity with two temperatures. Acta Mech. 2004;168:61–73.
[13] Youssef HM. Theory of two-temperature-generalized thermoelasticity. IMA J Appl Math. 2006;71:383–90.
[14] Jadhav N, Gaikwad K, Khavale S. Fractional order thermoelastic problem for a thin circular plate with uniform internal heat generation. J Heat Mass Transf. 2023;35:107–24.
[15] Awad E, Alhazmi S, Abdou M, Fayik M. Anomalous thermally induced deformation in Kelvin–Voigt plate with ultrafast double-strip surface heating. Fractal Fract. 2023;7:563.
[16] Guo H, Shang F, Tian X, He T. An analytical study of transient thermo-viscoelastic responses of viscoelastic laminated sandwich composite structure for vibration control. Mech Adv Mater Struct. 2022;29:171–81.
[17] Guo H, Shang F, He T. Fractional-order rate-dependent piezoelectric thermoelasticity theory based on new fractional derivatives and its application in structural transient response analysis of smart piezoelectric composite laminates. Int J Appl Mech. 2024;16:2450016.
[18] Awad E. A note on the spatial decay estimates in non-classical linear thermoelastic semi-cylindrical bounded domains. J Therm Stresses. 2011;34(2):147–60. doi: 10.1080/01495739.2010.511942.
[19] Awad E, Dai W, Sobolev S. Thermal oscillations and resonance in electron–phonon interaction process. Z Angew Math Phys. 2024;75:143. doi: 10.1007/s00033-024-02277-w.
[20] Fan T. Mathematical theory of elasticity of quasicrystals and its applications. Springer: Singapore; 2016. doi: 10.1007/978-981-10-1984-5.
[21] Lotfy K, El-Bary A, Hassan W, Alharbi A, Almatrafi M. Electromagnetic and Thomson effects during photothermal transport process of a rotator semiconductor medium under hydrostatic initial stress. Results Phys. 2020;16:102983. doi: 10.1016/j.rinp.2020.102983.
[22] Lotfy K, El-Bary A, El-Sharif AH. Ramp-type heating microtemperature for a rotator semiconducting material during photo-excited processes with magnetic field. Results Phys. 2020;19:103338. doi: 10.1016/j.rinp.2020.103338.
[23] Lotfy K, El-Bary A, Hassan W, Ahmed MH. Hall current influence of microtemperature magneto-elastic semiconductor material. Superlattices Microstruct. 2020;139:106428. doi: 10.1016/j.spmi.2020.106428.
[24] Mandelis A. Photoacoustic and thermal wave phenomena in semiconductors. United States: Elsevier; 1987.
[25] Lotfy K, El-Bary A, Daoud S, Ahmed MH, Allan M. A novel model of nonlocal photoacoustic and plasmaelastic heated by laser pulsed excitation of nanoscale semiconductor medium. Phys Fluids. 2024;36:012021. doi: 10.1063/5.0190226.
[26] Alshehri H, Lotfy K, Raddadi M, El-Bary A. A nonlocal photoacoustic effect with variable thermal conductivity of semiconductor material subjected to laser heat source. Results Phys. 2024;61:107715. doi: 10.1016/j.rinp.2024.107715.
[27] Sadeghi M, Kiani Y. Generalized magneto-thermoelasticity of a layer based on the Lord–Shulman and Green–Lindsay theories. J Therm Stress. 2022;45:319–40.
[28] Abbas I, Marin M. Analytical solutions of a two-dimensional generalized thermoelastic diffusions problem due to laser pulse. Iran J Sci Technol Trans Mech Eng. 2018;42:57–71.
[29] Hobiny A, Abbas I. Theoretical analysis of thermal damages in skin tissue induced by intense moving heat source. Int J Heat Mass Trans. 2018;124:1011–4.
[30] Singhal A. Theoretical investigation of SH wave transmission in magneto-electro-elastic structure having imperfect interface using approximating method. Appl Phys A. 2024;130:597. doi: 10.1007/s00339-024-07744-9.
[31] Tiwari R, Saeed AM, Kumar R, Kumar A, Singhal A. Memory response on generalized thermoelastic medium in context of dual phase lag thermoelasticity with non-local effect. Arch Mech. 2022;74(2–3):69–88. doi: 10.24423/aom.3926.
[32] Singhal A. Examining three distinct rheological models with flexoelectric effect to investigate Love-type wave velocity in bedded piezo-structure. Z Angew Math Mech. 2024;104:e202400724. doi: 10.1002/zamm.202400724.
[33] Gupta V, Barak M. Photo-thermo-piezo-elastic waves in semiconductor medium subject to distinct two temperature models with higher order memory dependencies. Int J Numer Methods Heat Fluid Flow. 2024;34(1):84–108. doi: 10.1108/HFF-07-2023-0380.
[34] Gupta V, Barak M, Ahmad H. Reflection of quasi plasma wave in photo-piezo semiconductor medium with distinct higher order

fractional derivative two temperature models. Phys, Scr. 2024;99:025515. doi: 10.1088/1402-4896/ad1972.
[35] Barak M, Ahmad H, Kumar R. Behavior of higher-order MDD on energy ratios at the interface of thermoelastic and piezothermoelastic mediums. Sci Rep. 2023;13:17170. doi: 10.1038/s41598-023-44339-5.
[36] Othman M, Fekry M, Marin M. Plane waves in generalized magneto-thermo-viscoelastic medium with voids under the effect of initial stress and laser pulse heating. Struct Eng Mech. 2020;73(6):621–9.
[37] Maldague XP, Zhang SY. Introduction to the scope and applications of photothermal and photoacoustic effects, Photothermal and Photoacoustic Phenomena II. Vol. 11, Bellingham, Washington, USA: International Society for Optics and Photonics; 1992.
[38] Gutiérrez-Reyes E, García-Segundo C, García-Valenzuela A, Ortega R, Buj C, Filbir F. Heat transport considerations in the mathematical analysis of the photoacoustic and photothermal effects. J Phys Commun. 2019;3:085007.
[39] Marin M. An evolutionary equation in thermoelasticity of dipolar bodies. J Math Phys. 1999;40(3):1391–9.
[40] Marin M. On existence and uniqueness in thermoelasticity of micropolar bodies. Comptes Rendus l'Académie Sci, Paris, Série II. 1995;321(12):475–80.
[41] Abouelregal A, Alhassan Y, Althagafi H, Alsharif F. A two-temperature fractional DPL thermoelasticity model with an exponential Rabotnov kernel for a flexible cylinder with changeable properties. Fractal Fract. 2024;8:182.
[42] Ailawalia P, Sachdeva S, Pathania D. Two-dimensional problem on laser pulse heating in thermoelastic microelongated solid. Arch Thermodyn. 2019;40(2):69–85.
[43] Abo-Dahab S, Abouelregal A, Marin M. Generalized thermoelastic functionally graded on a thin slim strip non-Gaussian laser beam. Symmetry. 2020;12(7):1094.
[44] Lata P, Kaur H. Interactions in a transversely isotropic new modified couple stress thermoelastic thick circular plate with two temperature theory. Coupled Syst Mech. 2023;12(3):261–76.
[45] Lata P. Thermomechanical interactions in a transversely isotropic thermoelastic media with diffusion due to inclined load. Struct Eng Mech. 2024;90(3):263–72.
[46] Kaur I, Singh K. Effect of memory dependent derivative and variable thermal conductivity in cantilever nano-beam with forced transverse vibrations. Forces Mech. 2021;5:100043.
[47] Kaur I, Lata P, Singh K. Thermomechanical deformation in a transversely isotropic magneto-thermoelastic rotating solids under initial stress. Partial Differ Equ Appl Math. 2021;3:100028.
[48] Ailawalia P, Priyanka, Marin M, Altenbach H. Variable thermal conductivity in context of Green-Naghdi theory of thermo-microstretch solids. ZAMM-J Appl Math Mech/Z Angew Math Mech. 2024;104(4):e202400010.